

# Energy Calibration of Underground Neutrino Detectors using a 100 MeV electron accelerator.

Sebastian White and Vitaly Yakimenko  
Brookhaven National Laboratory  
Upton, NY 11973 USA

April 20, 2010

## 1 Introduction

An electron accelerator in the 100 MeV range, similar to the one used at BNL's Accelerator test Facility (Table 1), for example, would have some advantages as a calibration tool for water cerenkov or Liquid Argon neutrino detectors. Alternatives like Michel electrons from cosmic ray muons and the low energy (5-16 MeV) linac used by Super Kamiokande don't cover the full energy range needed for the future long baseline program and have poor time definition.

In LBNE the electron neutrino energy distribution will be fit to obtain the CP violation parameter. One of the contributions to the energy scale (relative and absolute) uncertainty is the electron resolution function. An accelerator that allows for a scan of the electron energy over the range of 0.1 to a few GeV would be very important for this measurement. Our goal is to address absolute energy scale calibration up to an electromagnetic shower energy of at least 1 GeV.

Super Kamiokande's linac intensity was reduced from  $10^6$  electron/pulse to 1 electron/pulse using constraints on the beam divergence and momentum spread. The pulse width was 1-2  $\mu\text{sec}$ .

Here we investigate large angle Mott scattering as a technique to reduce the beam intensity to  $\sim 1/2$  electron/pulse. Since it is difficult to operate electron accelerators at  $\leq 10^7$  e/pulse we need this level of reduction. This is also potentially an attractive way to produce a benchtop secondary beam.

It would seem that this scheme could only work if the primary beam can be brought close to the detector. However a focusing triplet with a length of 0.5 meters and 2 centimeter aperture could be placed at 0.5 to 1 meter from the scattering target thereby extending this distance by at least a factor of 10.

In this note we calculate the thickness of targets that would be needed to produce a scattered beam of  $1/2$  electron/pulse and the amount of emittance growth they would

produce in the beam downstream of the target. If the multiple scattering is small enough it should be possible to have many secondary beam ports along the length of the accelerator.

Surprisingly we find that the beam emittance blowup caused by the scattering target doesn't depend very much on the choice of material in spite of the very strong contribution of the form factor. So the conclusion of our optimization exercise is that there isn't really an optimum choice of target. But lighter targets are better than gold.

This technique could provide several energy calibration points. At large angles, depending on the target material, well resolved inelastic peaks with a typical 4 MeV spacing, corresponding to the nuclear level structure, appear in the scattered electron energy spectrum, as seen in Figure 4. The energy resolution of the Icarus[3] detector is roughly 4% at 100 MeV. A water Cerenkov detector with 25% coverage would have a  $\sim 4.5\%$  stochastic term at this energy.

With this technique one could also take advantage of the strict proportionality between the accelerator intensity and the scattered electron multiplicity in a pulse. The beam intensity in the ATF, for example, can easily be adjusted over a range of more than  $\times 10$  and it is well measured so it would be straightforward to vary the mean energy deposit within a pulse shorter than 1 nsec from the beam energy to  $\sim 10$  times the beam energy. Icarus[3] shows that there are different problems in analyzing high energy showers compared to low energy showers but multiple electron showers have also been used in calibrations- for example at the Final focus testbeam.

For some purposes it could be useful that, because of statistical fluctuations in the electron multiplicity, one can simultaneously measure the response in several energy peaks as illustrated in fig. 5.

We will return to the question of construction and operating costs.

Table 1: An example: ATF parameters

Beam Energy	80 MeV
Bunch Intensity	$10^8 - 10^{10}$ e/pulse
Rep Rate	1 Hz
Bunch Length	3 picoseconds
Length	60 ft.
Power Consumption	10 kW

## 1.1 Scattered rates

We calculate the scattered electron rate starting from the Mott scattering formula (eqns. 1-5). The term  $\propto Z\alpha_{EM}$  in eqn. 2 is often not included but becomes significant above  $Z \simeq 6$ . For all targets we consider the form factor suppression is significant, even at this low energy. Hofstadter's measurements were taken with beams in the 100 MeV energy

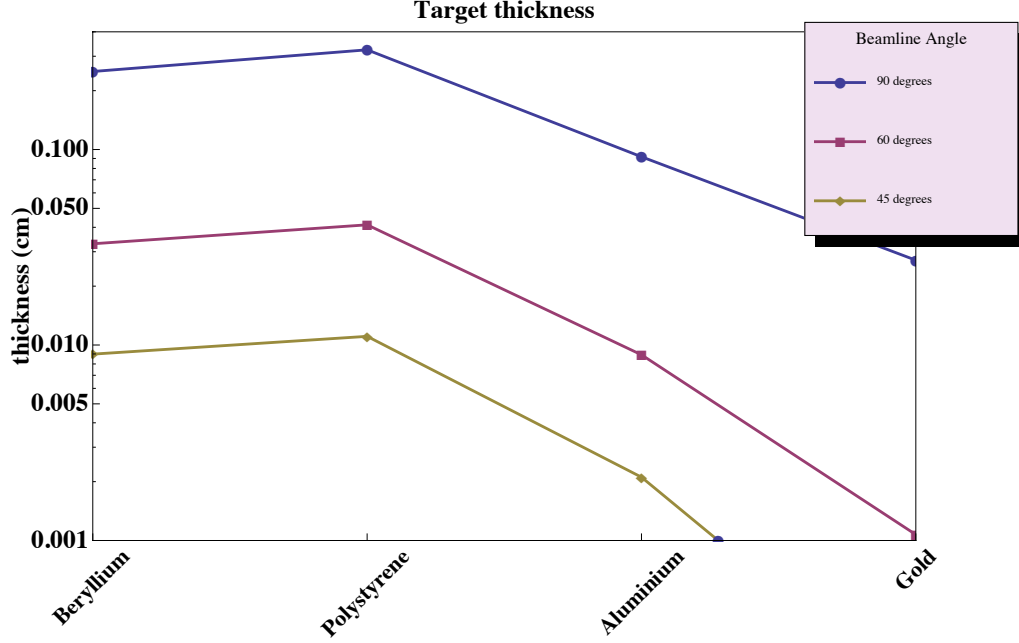


Figure 1: Calculated thickness (in centimeters) of scattering foils needed to produce 0.5 scattered electron/pulse in an aperture of  $1^0$  or  $10^{-3}$  steradians.

range. It has been useful to compare this calculation with his cross section measurements- particularly Be-120 MeV, H and C-187 MeV, Au- 84 MeV.

To parametrize the form factors we follow Hofstadter's original formula (eqn. 3-4). In this formula the charge density profile is fitted with an exponential form and the slope parameters are given in his papers (see Table 2). The slope parameter,  $a$ , is defined by  $r=2a\sqrt{3}$ , where  $r$  is the charge radius. Since the  $A^{1/3}$  form doesn't fit the radii of lighter nuclei there isn't an obvious way to calculate it so we use his measured values.

In this problem, since we require a scattered rate of 1/2 event/pulse, we invert the usual expression for the rate (i.e.  $\text{rate} = \text{flux} \times \sigma \times \rho \times t$ ) to find the target thickness,  $t$ , needed to get this rate.

$$\left(\frac{d\sigma}{d\Omega}\right)_{\text{Rutherford}} = 1/4(Z \cdot \alpha_{EM})^2 \frac{(\hbar c)^2}{E_e^2} \text{Cosec}(\theta/2)^4 \quad (1)$$

$$(\frac{d\sigma}{d\Omega})_{Mott} = (\frac{d\sigma}{d\Omega})_{Rutherford} \cdot \cos(\theta/2)^2 (1 + \frac{\pi Z\alpha_{EM} \sin(\theta/2)(1 - \sin(\theta/2))}{\cos(\theta/2)^2}) \quad (2)$$

$$\rho(r) = \frac{1}{8\pi(a)^3} \text{Exp}(-r/a) \quad (3)$$

$$\text{FormFactor}(Q) = \frac{4\pi \int_0^\infty r \rho(r, a) \sin(rQ) dr}{Q} \quad (4)$$

$$(\frac{d\sigma}{d\Omega})_{Hofstadter} = (\frac{d\sigma}{d\Omega})_{Mott} \text{FormFactor}(Q)^2 \quad (5)$$

Table 2: Slope parameter

	a(Fermi)	$r_0 A^{1/3} / (2\sqrt{3})$
Beryllium	0.64	0.780609
Carbon	0.69	0.859171
Gold	2.3	2.18361

We obtain good agreement with available data in Ref.[1] at several energies and for H through Au targets. This justifies the use of the exponential fit for the charge distribution.

In Fig. 2, for example, we show a comparison of this calculation with Hofstadter's data for gold. This calculation misses some of the diffractive fine structure seen with high energy beams but agrees everywhere to within a factor of 2.

The results for target thickness are shown in Fig 1 and also in Table 3.

Table 3: Calculated foil thicknesses (cm)

	Beryllium	Polystyrene	Aluminum	Gold
45 <sup>0</sup>	0.00898032	0.011074	0.00210775	0.000146681
60 <sup>0</sup>	0.0329445	0.0411883	0.00891158	0.00107188
90 <sup>0</sup>	0.250656	0.323623	0.0918123	0.0271518

## 1.2 Beam emittance

For the beam to be useful downstream of the scattering target it would be best to keep the target thickness to a minimum and reduce multiple scattering in the target. The nonprojected multiple scattering distribution is characterized by  $\theta_0$ , which is the standard deviation of the gaussian approximation for the forward beam spread, and can be expressed as

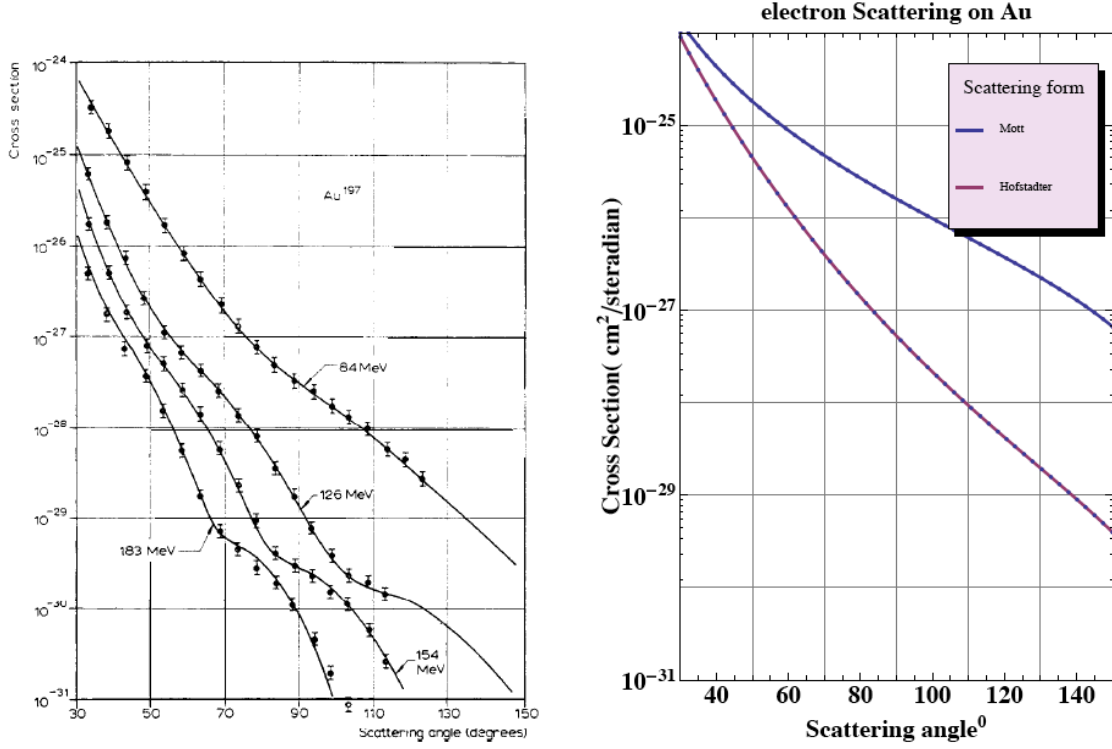


Figure 2: Elastic scattering data on Au at 84 MeV (upper curve) from Ref. [1](left) compared with this calculation (right). Also shown in the upper curves of this calculation are the cross sections obtained without form factor suppression.

$$\theta_0 = \frac{13.6 \text{ MeV}}{E_e} \sqrt{\frac{t}{X_0}} \cdot (1 + .038 \cdot \ln(\frac{t}{X_0})). \quad (6)$$

where  $t$ , the target thickness, and  $X_0$ , the radiation length of the material, are given in centimeters and the incident electron energy,  $E_e$  is in MeV. Foils thick enough to produce a scattered beam at  $90^\circ$  also lead to a significant emittance blowup ( $\theta_{MCS} \sim .7^\circ$ ) -see Fig 3 and table 4 while, with a  $45^\circ$  secondary beam, the multiple scattering angle in the primary beam is only  $\sim 0.1^\circ$ .

Since we find for light targets that  $t/X_0$  is smaller than  $\alpha_{EM}$  the line shape of scattered electrons is dominated by inner Bremsstrahlung and therefore has negligible distortion ( $dN_\gamma/dk \sim \alpha_{EM}/k$ ).

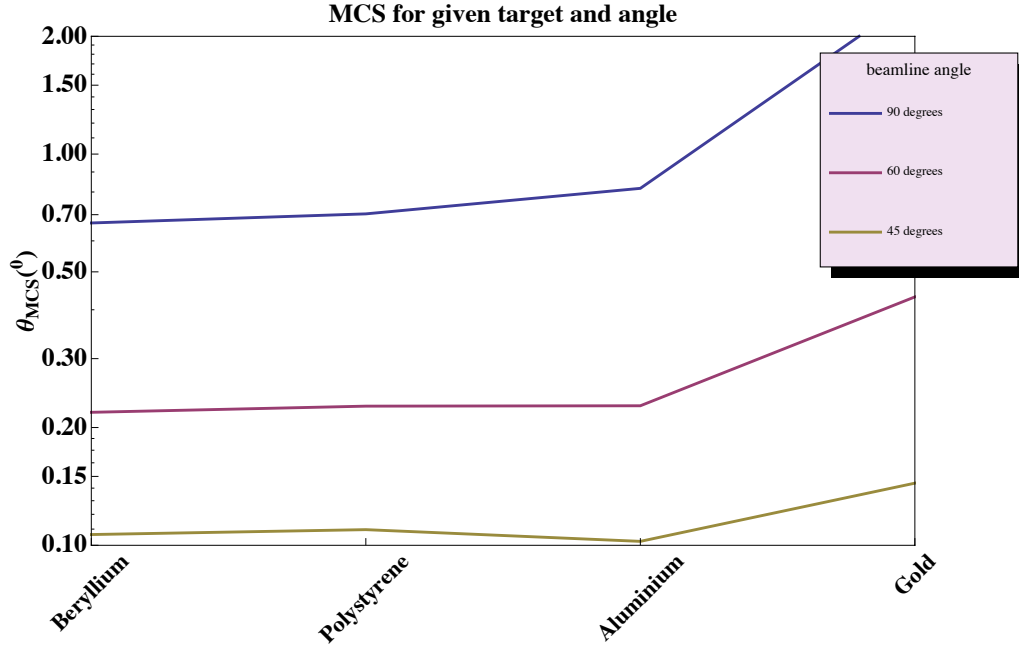


Figure 3: Multiple Coulomb scattering in the forward beam due to different choices of foil thickness.

### 1.3 Secondary peaks in the electron spectrum

One feature of this method is that for certain targets and scattering angles the electron spectrum has secondary peaks due to energy loss through excitation of nuclear levels. If the detector can resolve these peaks which in  $C^{12}$ , for example, have a spacing of 4.4 MeV, this would be a nice demonstration of performance.

The case of  $C^{12}$  is illustrated in Fig. 4 where the left panel shows the energy spectrum seen at an angle of  $80^\circ$  degrees. The right panel shows the angular dependence of elastic and inelastic cross sections at 187 MeV. At roughly 90 degrees the 1st inelastic peak and the elastic peak become equal.

### 1.4 Costs and Impact

We are looking at several approaches to costing this accelerator. There are a number of similar accelerators which are soon de-commissioning and it is clear that many components

Table 4: rms Multiple Coulomb Scattering Angle(<sup>0</sup>)

	Beryllium	Polystyrene	Aluminum	Gold
45 <sup>0</sup>	0.106529	0.109651	0.102343	0.144157
60 <sup>0</sup>	0.21874	0.226824	0.227326	0.431394
90 <sup>0</sup>	0.666669	0.703342	0.817344	2.51229

will become available for free. Below we list the component costs based on firm quotes in most cases. For example, the sections are from a SLAC design fabricated in China, the photoinjector quotes are from AES and RadiaBeam and the laser cost is from a 2009 quote to ATF.

The engineering and maintenance costs of a custom built accelerator could be significant. For example, assembly of the 100 MeV machine given in Table 5 would certainly require a year of work by an RF/laser engineer.

Another approach is to order a turn-key machine from one of 2 companies-AES on Long Island or RadiaBeam in Santa Monica, Ca. This solution could be completed in  $\sim 18$  months and would cost  $\sim 50\%$  more than the component cost given below[5].

Maintenance costs would depend a lot on the running scenario. Although such machines run at essentially 100% duty cycle, doing so assumes that there is a staff on hand to operate the machine- at least a technician and a laser engineer. If a lower duty cycle is needed and one can absorb unanticipated down times then you wouldn't need more than 1 person on staff.

Generally the impact on the infrastructure is the 10 kWatt continuous power required. This machine would have a  $\sim 600 \text{ ft}^2$  footprint and would be at least 30 ft long. For example, it could be 30ft x 20ft or 60ft x 10ft. For installation, the accelerator could be broken down into smaller modules with dimensions  $10 \times 6 \times 6 \text{ ft}^3$  (in any orientation) and lowered into DUSEL.

Table 5: rough Costs

Component costs	
TiSapphire Laser (ATF quote)	400k
Photoinjector (AES, Radia Beam)	350k
2 Klystrons	250k
2 Modulators	500k
2 Sections	300k
Low level RF, etc.	200k
Supports, etc.	100k
Total	2.1M USD

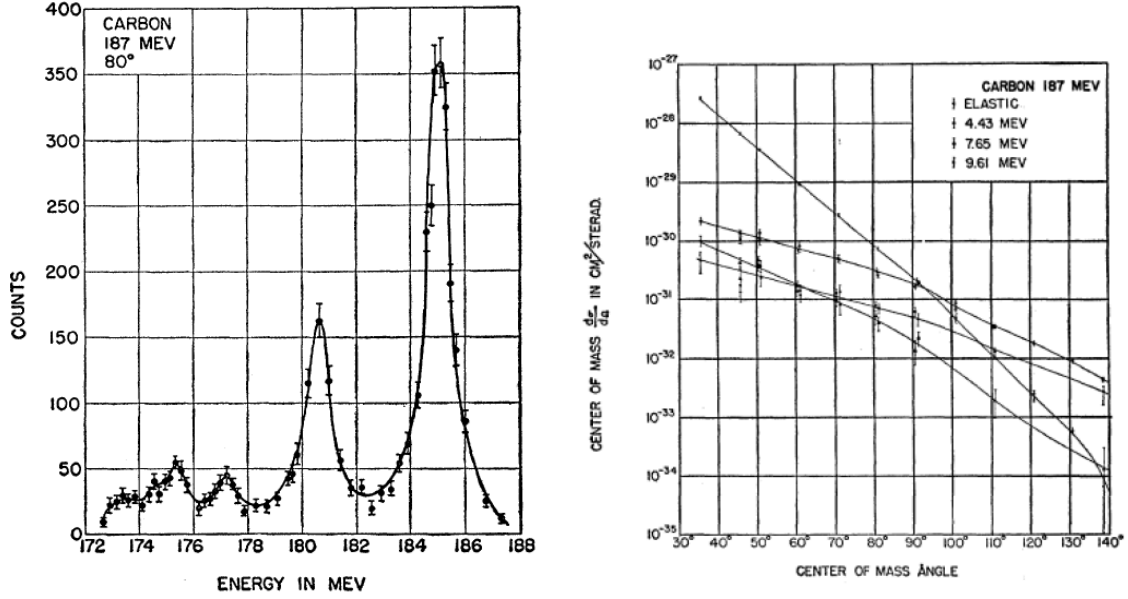


Figure 4: The left panel shows the energy spectrum seen at one angle ( $80^\circ$ ). This spectrum results from energy loss due to nuclear excitation since  $E_{scattered} = E_{beam} - E_{excitation}$ . The right panel shows the angular dependence of the elastic and inelastic rates.

## References

- [1] R. Hofstadter , Rev. Modern Physics **28** 3, 214 (1956).
- [2] M. Nakahata *et al.* (Super-K collaboration), [arxiv.org/abs/hep-ex/9807027](https://arxiv.org/abs/hep-ex/9807027).
- [3] A. Ankowski *et al.* (Icarus collaboration), [arxiv.org/pdf/0812.2373](https://arxiv.org/pdf/0812.2373).
- [4] E. Blucher *et al.*, DRAFT Report on the Depth Requirements for a Massive Detector at Homestake.
- [5] quotation from RadiaBeam Technologies, Jan. 27, 2010.



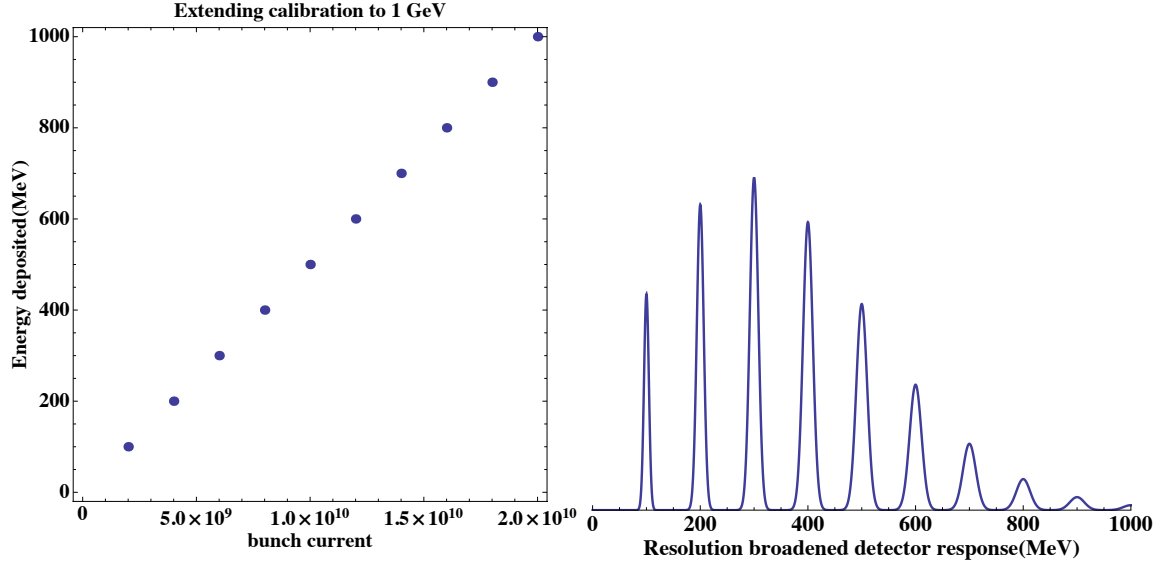


Figure 5: The scattered electron rate is linear in the primary beam intensity and this is well measured. So it will be straightforward to adjust the current to get, on average, an energy deposit of several times  $E_{beam}$ . The right plot shows schematically the expected energy response for a 100 MeV beam with intensity of  $8 \times 10^9$  electrons/pulse. The peaks are smeared assuming an energy resolution corresponding to photostatistics of 5 photoelectrons/MeV expected for a water Cerenkov detector with 25% coverage. The stochastic term for LAr obtained by Icarus[3] is somewhat better- ie  $\sim 0.33/\sqrt{E(MeV)}$ .